Mechanical characteristics of hydrogen-implanted crystalline silicon after post-implantation annealing

Suet To[1], Emil V. Jelenković[1], Lyudmila V. Goncharova[2], Sing Fai Wong[3]

[1] State Key Laboratory of Ultra-precision Machining Technology, Department of Industrial and Systems Engineering, The Hong Kong Polytechnic University, Hong Kong SAR, PR China

[2] Department of Physics and Astronomy, The University of Western Ontario, 1151 Richmond Street, London, Ontario, Canada, N6A 3K7

[3] A & P Instruments Co., Ltd. Room 68, 1/F Sino Industrial Plaza, 9 Kai Cheung Road, Kowloon Bay, Hong Kong SAR, PR China

Abstract

Knowing the mechanical properties of single crystal silicon after implantation with hydrogen and annealing are important for "smart cut" process and in improving ultra-precision cutting of silicon. There is limited information on hardness and modulus of such silicon. In this article, the effect of hydrogen implantation dose and post-implantation annealing on silicon hardness and modulus were investigated. Continuous implanted silicon layers, from the surface to the depth of ~500 nm, were produced. Samples with three different implantation doses and with post-implantation annealing at 350 ^{o}C and 400 ^{o}C were prepared. Hardness and modulus were obtained through dynamic nanoindentation, while structural properties were evaluated by Rutherford backscattering spectroscopy and high resolution x-ray diffraction. Hardness and modulus were significantly reduced after annealing for the highest implantation dose. With the annealing, the implantation-induced strain had the least relaxation for the lowest implantation dose. The obtained results could be useful for understanding the role of hydrogen in nano-cutting of hydrogen-implanted silicon.

Keywords: elastic modulus; hardness; silicon; hydrogen implantation; Rutherford Backcattering Spectroscopy; high resolution XRD;

1.Introduction

Hydrogen has significant technological importance in single crystal silicon in improving electrical performance of MOSFETs by terminating the dangling bonds at the interface gate oxide-silicon [1]. However, the focus in this article is a modification of the mechanical properties of silicon with hydrogen and it's effects on two applications. (i) Hydrogen is crucial in so-called "smart cut" process for silicon on insulators (SOI) technology [2-7]. In the latter, hydrogen implantation depth controls the desired thickness of the semiconductor layer in SOI structure. (ii) Silicon optical devices can be fabricated by ultra-precision machining. It is well known that Si is difficult to machine because of it's high hardness and brittleness. Recently, it was shown that implanted hydrogen can improve nano/micro machinability of silicon [8,9].

The "smart cut" process is possible only with the post-implantation annealing [2-7]. During the annealing, the implantation-induced defects are rearranged and platelets and molecular hydrogen accumulate at around ion projection range. These structural changes help the exfoliation of a thin silicon film on the insulator. On the other hand, in the plunge cut experiments on the post-implantation annealed silicon, some of the improvements in the machinability of silicon were reversed in the ductile mode of cutting [10]. But the cutting force was reduced with the annealing 300 at 400 ^{o}C in the brittle regime of cutting [10]. Therefore, the post-implantation annealing is very important for both the "smart-cut" and in sharp-tool cutting processes. It should be noted that in Ref. 10, the implantation scheme structurally affected silicon mainly at the depth of ~1.00-1.55 μm, which is far away from the ductile regime cutting of silicon [11].

The mechanical behavior of silicon in the "smart cut" process is well explained from the structural point of view. However, little is known about mechanical properties like hardness (H) and elastic modulus (E) of hydrogen-implanted silicon after annealing. To the best of our knowledge, there is one report on H and E of post-implantation annealed silicon [7]. In this report [7], it was shown that within the depth of implanted hydrogen (~400 nm) there was (i) no change in elastic modulus and hardness after implantation; (ii) after annealing there was significant reduction in hardness, while modulus was not reduced in the gross of the implanted region; and (iii) the changes were not related to the implantation dose. Our investigation of H and E on Si implanted with different hydrogen ion doses, demonstrated that hardness increases with the implantation dose, while the highest reduction of elastic modulus was obtained for the lowest implantation dose [12]. These results may suggest that in annealed samples H and E would be hydrogen dose dependent as well, which at the end may control both the "smart cut" process and the machinability of silicon.

In this report, hydrogen was implanted into silicon with different doses, creating implantation region from surface to the depth of ~500 nm, while thermal annealing temperature was selected to be below the silicon layer exfoliation temperature [7,13]. The mechanical properties of silicon were acquired through nanoindentation tests and were related to the structural properties obtained by Rutherford backscattering spectroscopy (RBS), high-resolution x-ray diffraction (HRXRD) and secondary ion mass spectrometry (SIMS). The implantation scheme was selected to cover the ductile cutting region of silicon [9,11].

2.Experimental

One side polished Si (001) wafers (10 cm in diameter) with the resistivity of 5-25 Ohm-cm were oxidized in a wet atmosphere at 1100 ^{o}C. The oxide thickness was 300 nm. All samples were implanted with hydrogen ions through the oxide with double energy, first with 75 keV and after that with 40 keV. For both implantation energies, the same implantation dose was applied. Samples with three different doses were prepared: 0.5×10^{16} cm^{-2} (sample A), 1.5×10^{16} cm^{-2} (sample B) and 4×10^{16} cm^{-2} (sample C). The reference sample OS was also oxidized but did not go through the implantation process. The quarters of A, B and C wafers were annealed at 350 and 400 ^{o}C in a nitrogen ambient for 60 minutes and were labeled as shown in Table 1. Before nanoindentation, the oxide was etched away in a diluted hydrofluoric acid (HF) solution.

The dynamic nanoindentation was done on 1 cm × 1 cm silicon pieces with a Berkovich tip, with up to 50 mN maximum load, using iNano indenter. A fused quartz standard of known hardness and modulus was applied as a reference to monitor the performance of the nanoindenter system. The indenter's control program can automatically calibrate the tip area function and the load frame stiffness. Such calibrations are carried out according to the procedures proposed by Oliver et al. [14]. The physical characterizations were performed with HRXRD (Empyrean (PANanalytical) and RBS and SIMS. The wavelength of XRD system's x-ray was 1.5405980 Å. RBS measurements were conducted using He^{+} beam at energy of 3.0 MeV and the scattering

angle was 170 degrees in Cornell geometry. A Sb-implanted amorphous Si sample with a known Sb content of 4.82 $\times 10^{15}$ atoms/cm^2 was used to calibrate the detector solid angle. Spectra were fitted using SIMNRA [15] to determine the elemental composition and film thickness and to explore crystalline and amorphous regions.

Table 1. Processing conditions of samples

H^+ implantation energy	H^+ implantation dose (cm^{-2})	Sample name	Annealing temperature (^oC)	Annealing time (min)
-	-	OS	-	-
E1 = 75 keV E2 = 40 keV	D1=0.5x10^{16} D1=0.5x10^{16}	A	-	-
		A3	350	60
		A4	400	60
E1 = 75 keV E2 = 40 keV	D1=1.5x10^{16} D1=1.5x10^{16}	B	-	-
		B3	350	60
		B4	400	60
E1 = 75 keV E2 = 40 keV	D1=4x10^{16} D1=4x10^{16}	C	-	-
		C3	350	60
		C4	400	60

3. Results and discussion

The main concerns in this article are the changes in mechanical parameters (hardness and elastic modulus) after post-implantation annealing. These concerns are important since it was observed that the cutting properties of hydrogen-implanted silicon could be affected by low-temperature annealing, observed by the same authors on silicon implanted with hydrogen under different implantation scheme than in this article [10]. In order better to understand the changes in mechanical properties of hydrogen-implanted silicon after thermal annealing, only a brief analysis of post-implantation H and E is given in this article. Details of this analysis can be found in the published work by the same authors [12].

In this section, using channeling RBS, high resolution XRD and SIMS profiling of implanted hydrogen were used with the aim to explain the changes in H and E after post-implantation annealing.

3.1 Hardness and elastic modulus after annealing

The maximum penetration depth of nanoindentation was about 500 nm for all investigated samples. This depth is close to the tail of the ion and defect distribution of the implemented implantation scheme and was predicted using SRIM (Stopping Range Ions in Matters) [16] and was given in appendix A of this article.

The impact of hydrogen dose and annealing temperature on the change of hardness and modulus are illustrated in Figs. 1-6. In these figures, all curves present an average of 10 dynamic nanoindentation measurements. The change in hardness and modulus were calculated against the average hardness and modulus of OS sample, based also on 10 nanoindentation measurements and were 12.8 GPa and 176.9 GPa respectively. Details of average H and E calculations of OS sample are given in appendix B.

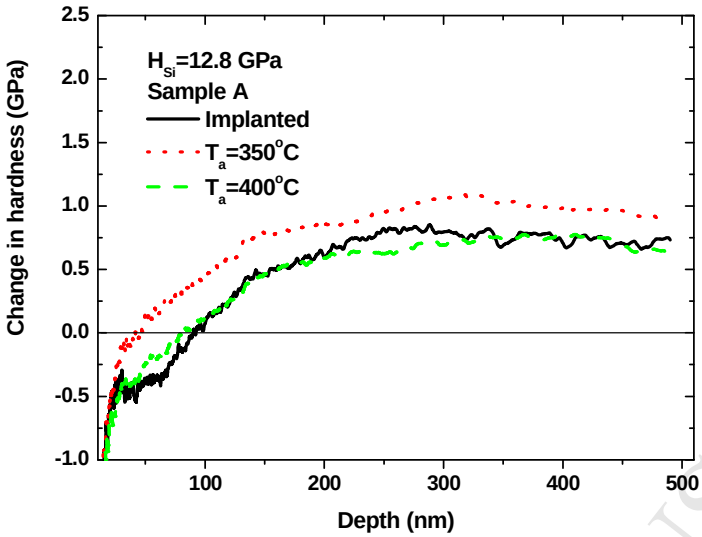

Fig.1. Change in hardness of sample A after implantation and annealing at 350 ^{o}C and 400 ^{o}C.

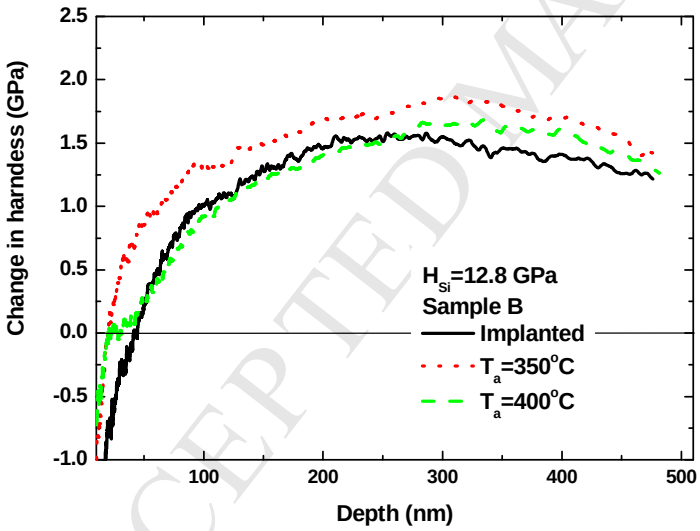

Fig.2. Change in hardness of sample B after implantation and annealing at 350 ^{o}C and 400 ^{o}C.

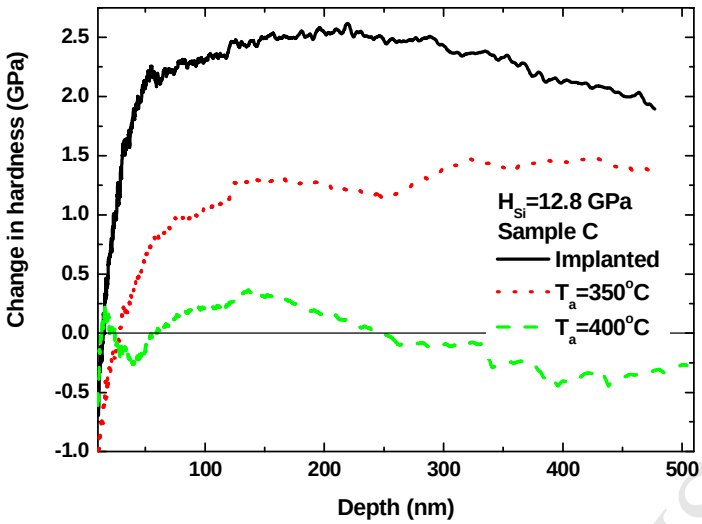

Fig.3. Change in hardness of sample C after implantation and annealing at 350 °C and 400 °C.

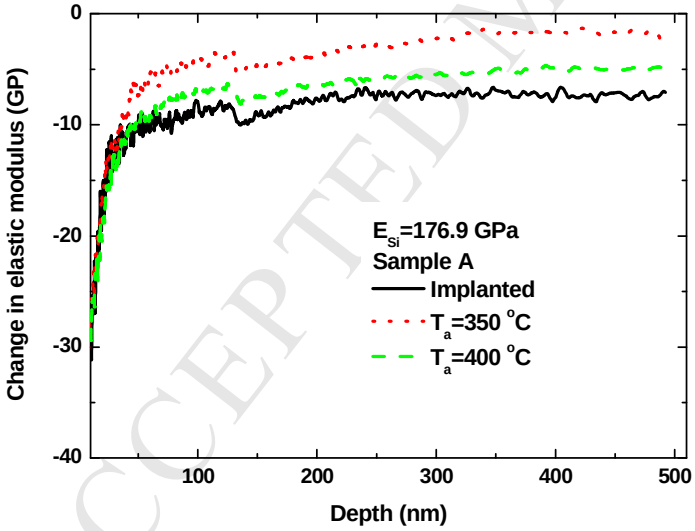

Fig.4. Change in elastic modulus of sample A after implantation and annealing at 350 °C and 400 °C.

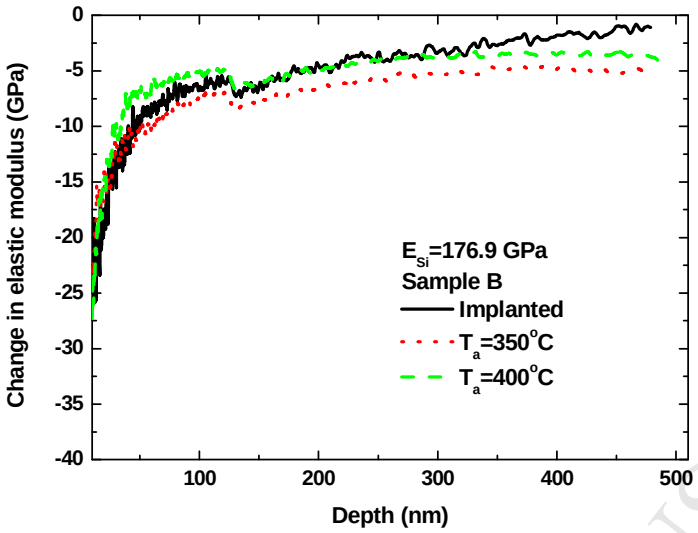

Fig.5. Change in elastic modulus of sample B after implantation and annealing at 350 °C and 400 °C.

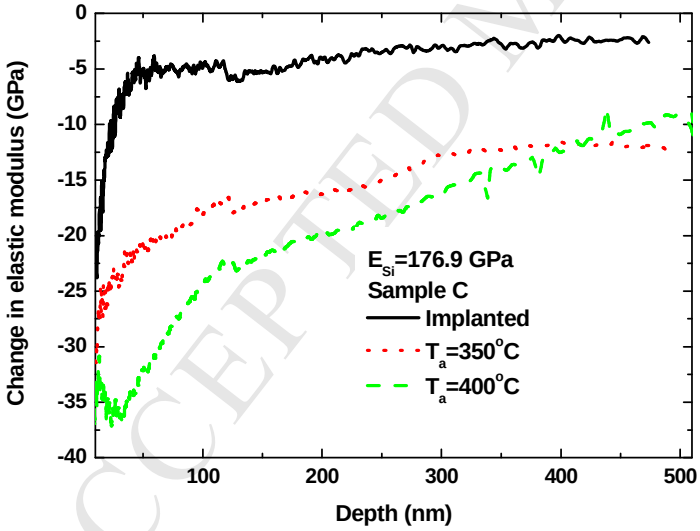

Fig. 6. Change in elastic modulus of sample C after implantation and annealing at 350 °C and 400 °C.

In all implanted samples, the change in hardness peaks at around 250 to 300 nm. The largest change in hardness for A, B and C samples were 0.8, 1.8 and 2.6 GPa, respectively. The increased hardness by implantation is also observed in the surface region up to 100 nm depth for all three implantation doses. However, we consider that the data for the depth of 0-30

nm are inaccurate based on the calibration of the nanoindentation system with a fused quartz standard [12]. The rise of hardness in OS sample at the depth of ~30-100 nm could be caused by the defects generated during wet oxidation. For instance, generation of stacking faults happens at 1100 ^{o}C during oxidation of silicon wafers in steam ambient [17]. This speculative explanation needs a special investigation.

It should be noted that obtained values of H (12.8 GPa) and E (177.9) of OS sample are close to the values for silicon published by Chang et al. [18]. Therefore, it can be assumed that the oxidation did not affect hardness and modulus and the results for OS can be used to compare these parameters with the same of implanted and annealed samples. The averaging of hardness and modulus based on multiple measurements was performed because it is known that in nanoindentation characterization of silicon there is some scattering in the load-unload curves, resulting in variation in mechanical properties [18] and randomness in pop-out appearance [19].

The modulus experiences less significant change after the hydrogen implantation. At around 250 nm, its reduction is in the range of 2 % for B and C samples and about 4 % for A sample. For partially damaged silicon with Ar ions, a reduction in E is observed within 6.5 to 11 %, depending on the implantation dose [20]. However, with full amorphization of silicon through Ar ion implantation, the largest reduction of E was about 20 % [20]. A similar reduction of E, 19 %, was obtained on an amorphous silicon layer produced by self-ion implantation into crystalline silicon [21]. Based on SRIM simulation, the implantation-induced damage to silicon in this work is below amorphization level of silicon and the observed 2-4 % reduction in modulus is considered reasonable in the light of used references [20,21]. At the depth of about 110-130 nm, a spike in E is observed in the studied samples. Such spiking was not seen on the standard fused quartz, and its origin is unknown [12]. A detailed analysis of H and E dependence on implantation dose are given in the previous publication by the same authors [12].

With annealing at 350 ^{o}C hardness is increased by about 0.5 GPa for samples A3 and B3, while there is a drop in the range of 0.5 to 2 GPa for sample C3. After annealing at 400 ^{o}C, hardness returned to about post-implantation hardness levels for samples A4 and B4 (Figs. 1 and 2), but for C4 sample it was reduced by 0.5 GPa from the reference OS sample value. In the report of Gu at al. [7], from Fig.3 (b) it can be observed that in fact the hardness was almost 14 GPa for unspecified implantation dose and was reduced to about 12 GPa after annealing at 400 ^{o}C. In the same report, the hardness of not implanted silicon was 12.9 GPa, like in our article. Gu et al. [7] missed interpreting a relation between hardness (and modulus) and the implantation dose. In that report [7], the reduction of hardness to about 12 GPa is likely due to longer annealing time of few hours in comparison to 60 minutes in this article.

The modulus for A3 sample slightly rebounded after annealing at 350 ^{o}C, while for A4 sample it was reduced to the value higher than after implantation (Fig.4). For B3 sample the modulus is marginally reduced and for B4 sample it returned to about the post-implantation value (Fig.5). With the annealing, samples C3 and C4 show a dramatic drop in E value and the decrease is especially significant in the region of ~30-100 nm for both annealing temperatures (Fig.6). This region, as it will be seen later, is away from the peaks of hydrogen and defect depth profiles. However, Gu et al. [22] also observed a greater reduction in modulus in the region of lower hydrogen concentration, and presumably, lower defect concentration. Again, as for the hardness, Gu et al. [7,22] did not link the observed modification of modulus before and after annealing with the implantation dose.

3.2 Hydrogen depth profile

It is known that hydrogen can improve the motions of dislocation in silicon exposed to hydrogen plasma [23]. Also, Xiao at al. [9] interpreted some of the improvements in the cutting

of hydrogen implanted silicon with the reduced reaction between certain sleep systems to the presence of hydrogen. Therefore, it is useful to know the concentration profile of hydrogen before and after annealing in order better to understand H and E behaviour described in this article. In Fig. 7, the hydrogen profile is shown for samples C and C4, but it is expected to be rather similar for other implantation doses because of the nature of the implantation process [12]. It should be noted that the vertical axis in Fig. 7 is in arbitrary units. No one curve for H and E in Figs. 1-6 for implanted silicon and implanted-annealed Si shows depth profile similar to hydrogen concentration profile in Fig. 7. This insensitivity of nanoindentation to the doping profile is demonstrated also for silicon irradiated with Kr [24]. The same reference showed also that hardness weakly follows the profile of implantation-induced defects.

The positions of the hydrogen peaks for C4 sample after implantation are at around 195 and 410 nm. With the annealing, they are moved deeper into silicon by about 10 and 30 nm respectively.

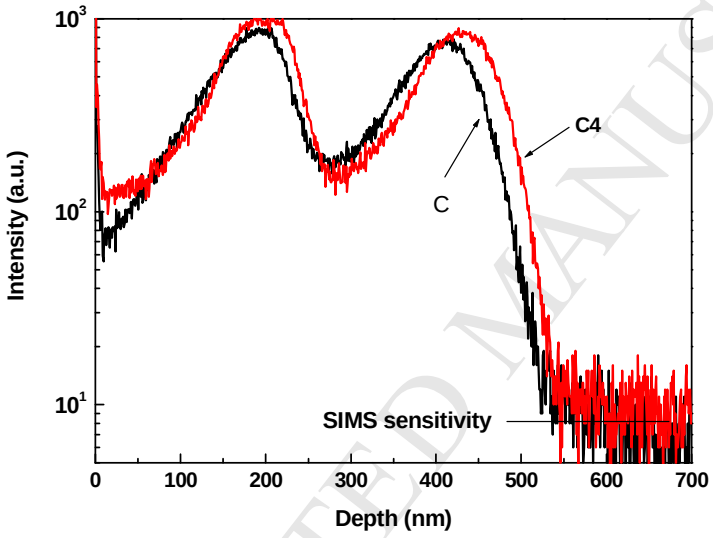

Fig.7. Hydrogen depth profile for implanted Si obtained by SIMS before annealing (sample C) and after annealing at 400 ^{o}C (sample C4).

3.3 Relation of hardness and modulus to silicon lattice damage

In hydrogen implanted silicon numerous defects are formed, including vacancies and Si-H complexes [2-7,13]. With the annealing, Si-H bonds are broken and hydrogen tends to move toward the hydrogen concentration peak [2-7], leading to platelets formation and H_2 accumulation [2-7,13] and overall to silicon reduced crystallinity which can be efficiently characterized by channeling RBS. The channeling spectra for implanted samples before and after annealing at 400 ^{o}C are given in Fig. 8. In the same figure, a random spectrum is given for A sample. The random spectra for the other samples are the same and are not included in the figure.

A partial reduction in crystallinity of implanted and annealed samples, except for sample A, was detected with channeling RBS (Fig. 8). While SRIM simulation points out that the crystalline lattice damage for the dose of 0.5×10^{16} cm^{-2} exists as well, the used RBS system was not sensitive enough to detect it.

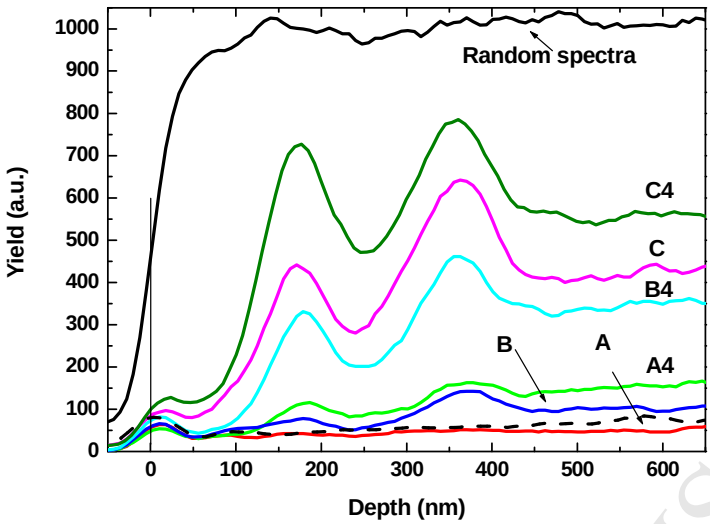

Fig.8. Ion yield distribution profiles for hydrogen implanted samples before (A, B, C) and after annealing at 400 ^{o}C (A4, B4 and C4). The dash line corresponds to the channeling spectrum of OS sample.

The increase in ion yield is proportional to defect density: we observe systematic increase in ion yield with an increase in H implantation dose in RBS channeling spectra. Two defect-related peaks are observed in Fig. 8, at about 170 and 370 nm. They are shifted by about 25 and 40 nm from the corresponding hydrogen peaks. This shift is in good agreement with the reported values of Nastasi et al. [5] who investigated single energy implantation of hydrogen in silicon.

In Fig.8, it can be noticed that with the annealing, the ion yield was increased in the region up to 100 nm as well. In this region, for sample C4 a steep drop in modulus is observed after annealing (Fig.6), while for samples A4 and B4 the modulus is either slightly increased or is unchanged in comparison to the implanted samples. The breaking of Si-Si bonds is supposed to lead to the reduction in modulus, as in the case of partial damage by argon implantation [20] or full amorphization by silicon and Kr implantation [21,24]. For C4 sample, in the region of 30-100 nm, the broken Si-Si bonds should be less in number than around the peaks in Fig. 8. Still, the reduction in modulus is greater than in the rest part of the hydrogen implanted layer. Obviously, there are other factors that influence the modulus, which may depend on the history of prepared silicon which will be illustrated with several examples. From the past reports, for instance, in an apparently step-like amorphous silicon (a-Si) layer obtained by Kr implantation into crystalline silicon, the modulus continuously grows from the surface of the layer to the value of bulk Si at the end of the step [24]. Regarding the hardness, in a-Si film obtained by silicon implantation into silicon, with later hydrogen implantation, hardness is reduced [25]. On the other hand, in sputtered a-Si, followed by hydrogen injection from plasma, hardness is increased [26].

3.4 Strain in implanted and annealed samples

In silicon implanted with hydrogen, a vertical strain is developed and it grows with the implantation dose [2-6]. With the annealing, along with the redistribution of implantation-induced defects and new defects formation, the relaxation of vertical strain happens as well [10,27]. HRXRD is a sensitive tool to detect this strain and was applied in this investigation.

In Figs.9, 10 and 11, high-resolution scan around Bragg plane (004) for samples A-A3-A4, B-B3- B4 and C-C3-C4 are given, respectively. The presence of fringes on the left side of the main peak indicates the existence of vertical strain. The left-most fringe corresponds to the highest strain of the implanted layer [6] and this statement will be sufficient to qualitatively analyze the role of hydrogen concentration and the annealing on the vertical strain. In order better to visualize the fringes after annealing, the left-most fringes of samples B and C are not shown. For these samples the left-most fringes are at 68.69 ^{o} and 67.88 ^{o}, respectively. The HRXRD of OS sample is shown in Appendix C. The fringes cannot be seen in this figure, indicating that OS sample is strain free.

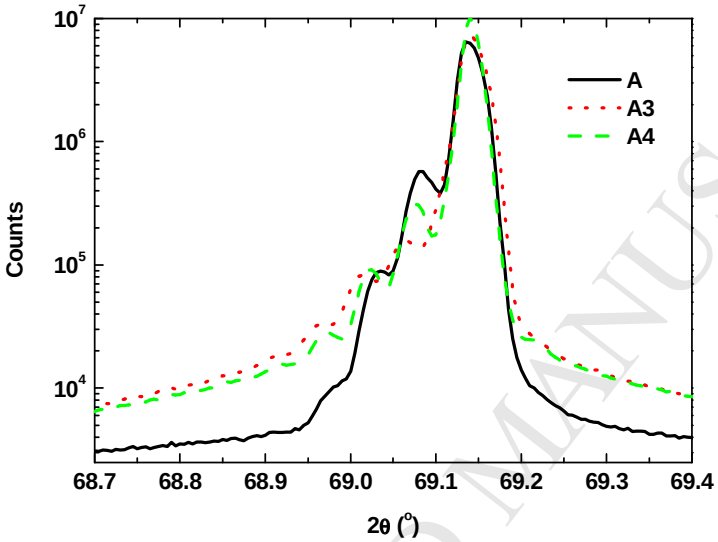

Fig. 9. High resolution XRD of A, A3 and A4 samples.

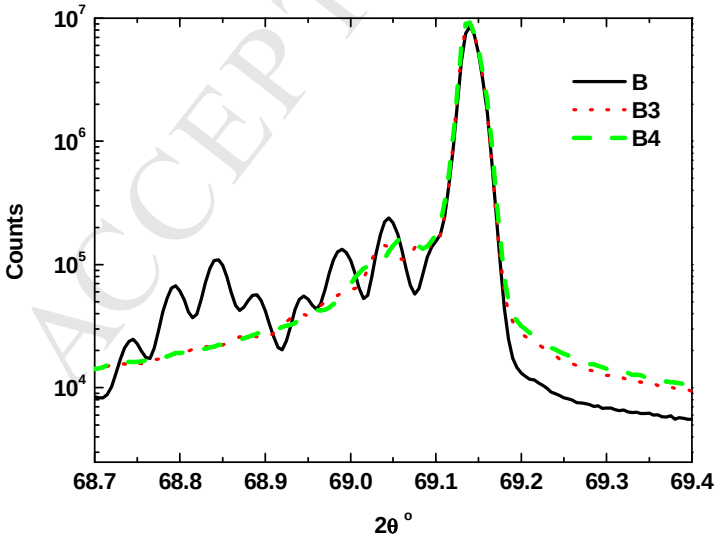

Fig. 10. High resolution XRD of B, B3 and B4 samples.

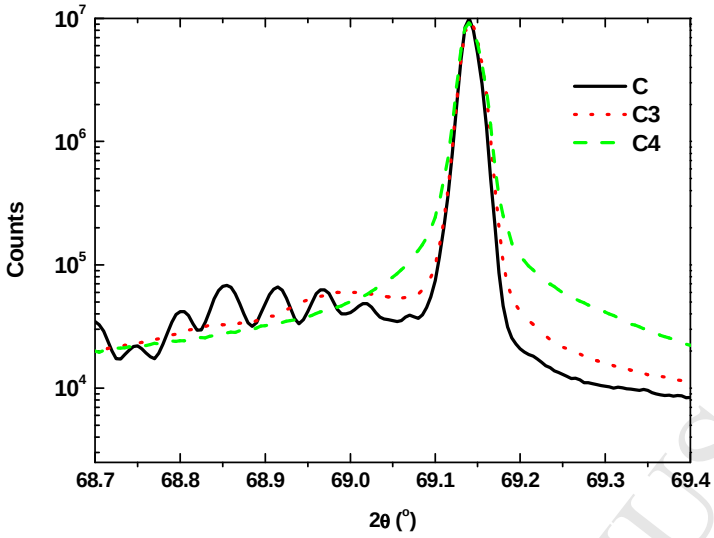

Fig. 11. High resolution XRD of C, C3 and C4 samples.

With the annealing, the fringes disappear for C4 sample and are partially eliminated for samples B3, B4 and C3. The remained fringes of B3, B4 and C3 sample are also moved to the most significant peak position at 69.14 ° which was recorded for OS sample (appendix C). These mean that the strain in B3, B4 and C3 is reduced in comparison to B and C samples, while in C4 sample the strain is fully eliminated. For C3 and C4 there is both reduction in hardness and modulus after annealing (Figs.3 and 6 respectively). The remained strain for sample B4 after annealing coincides with the observation that for this sample the hardness and modulus are returned to the post-implantation values. This is not the case with the set A-A3-A4, because of which a more detailed analysis of the left-most fringe for A samples was performed.

In Table 2, for the sample with $D=0.5\times10^{16}$ cm^{-2}, the position of 2θ is tabulated with the related average change in hardness and modulus before and after annealing. The changes in H and E in Table 1 are in reference to OS sample. A negative sign of E indicates a reduction of its value from the reference sample.

Table 2. Comparison of left-most fringe 2θ angle with the change of H and E.

Sample	Left-most peak position of 2θ (°)	Change in hardness (GPa)	Change in elastic modulus (GPa)
A	68.97	0.8	-7
A3	68.90	1.0	-2.3
A4	68.92	0.7	-5.2

The annealing at 350 °C introduces more strain in the sample as the left-most fringe has the 2θ angle moved from 68.97 to 68.90 °, which is reflected on the increase in hardness and a rebound in modulus (Table 2). With the annealing at 400 °C, the most left fringe 2θ value increases to 68.92 °, which corresponds to the decrease of hardness and modulus. These findings indicate that in addition to crystalline damage, vertical strain plays a role in mechanical properties of silicon. Miclaus et al. [27] observed that there was a shift to lower 2θ after annealing silicon

implanted with hydrogen at 150 ^{o}C for 10 and 30 minutes. However, Miclaus et al. [27] assigned their observation to the areal variation. Based on above our finding, it is proposed that for certain low hydrogen implantation doses and annealing temperatures, defect generation happens in silicon during the post-implantation annealing, which increases the tensile stress. In contrast, at certain high implantation dose (in our case D=1.5x10^{16} cm^{-2} and D=4×10^{16} cm^{-2}) and higher annealing temperature (400^{o}C) the annihilation of vertical strain is more efficient. These new findings may have an impact on the optimization of ultra-precision cutting of silicon modified by hydrogen implantation and will be studied in the future.

In the analysis of post-implantation annealing impact on H and E, the residual role of hydrogen in eventual post-cutting optical/electronic device is not mentioned. At this stage, we can only speculate that with annealing at temperatures higher than 700 ^{o}C the implanted hydrogen can be eliminated [29].

4. Conclusion

In this article, the hardness and modulus of silicon, after implantation of hydrogen with three different doses and post-implantation annealing at 350 and 450 ^{o}C, were investigated. The mechanical parameters were extracted after dynamic nanoindentation measurements. Main conclusions are:

(i) The hardness increases after annealing at 350 ^{o}C and decreases after annealing at 400 ^{o}C for lower implantation doses and is reduced for both annealing temperatures for D=4x10^{16} cm^{-2}.

(ii) The modulus is much affected and further reduced for both annealing temperatures only for D=4x10^{16} cm^{-2}.

(iii) The depth profiles of the changes of hardness and modulus with annealing do not follow the shape of the concentration profile of implanted hydrogen and defects distribution.

(iv) Annealing of silicon implanted with hydrogen diminishes the crystallinity of silicon. However, this is not the only reason that governs the mechanical properties of silicon and more investigation is needed in this direction.

(v) The hydrogen implantation-induced vertical strain is annihilated with different rates with the annealing and depends on implantation dose.

The results obtained in this study are expected to be useful for the future taper cutting of silicon modified by hydrogen implantation.

Acknowledgment: The work described in this paper was partially supported by the Research Committee of The Hong Kong Polytechnic University project (G-YBEX and BBX5). We would like to acknowledge the technical expertise of Mr. Jack Hendriks at Western Tandetron Accelerator Facility. This research was supported by the Natural Science and Engineering Research Council (NSERC) of Canada, and the Canadian Foundation for Innovation (CFI). The authors wish to thank A & P Instruments Ltd. Hong Kong for the use of iNano indenter.

Appendix

A. SRIM simulation

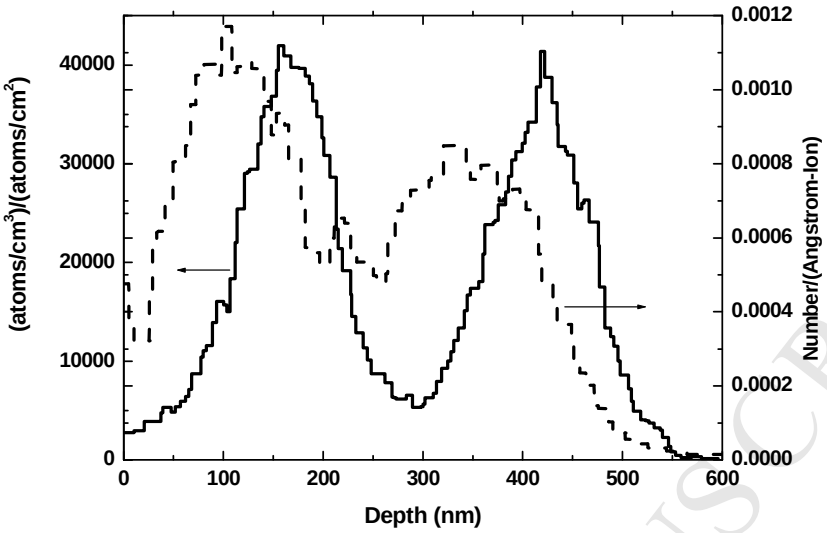

Fig.A SRIM simulation of hydrogen ion implantation into silicon through 300 nm thick SiO_2.

The full line represents ion distribution, while the dashed line represents vacancy distribution. The simulation was carried out with quartz SiO_2. The simulation with wet oxide density of 2.1 gcm^{-3} [28] did not change significantly the two distributions.

B. Determination of average hardness and elastic modulus of OS sample

Ten dynamic nanoindentation measurements were made on OS sample in order to find its average silicon hardness (H) and elastic modulus (E). Typical depth profiles for H and E are plotted in Fig.B. For each measurement H and E were averaged in the range from 100 to 500 nm. Afterwards, ten depth-related averaged values were averaged to give H=12.8 GPa and E=176.9 GPa for OS sample.

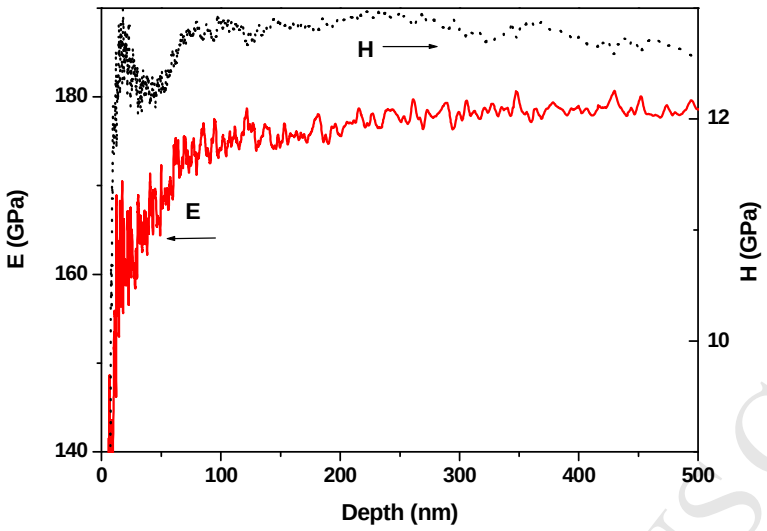

Fig.B Typical depth profiles for H and E of OS sample.

C. High resolution XRD of sample OS

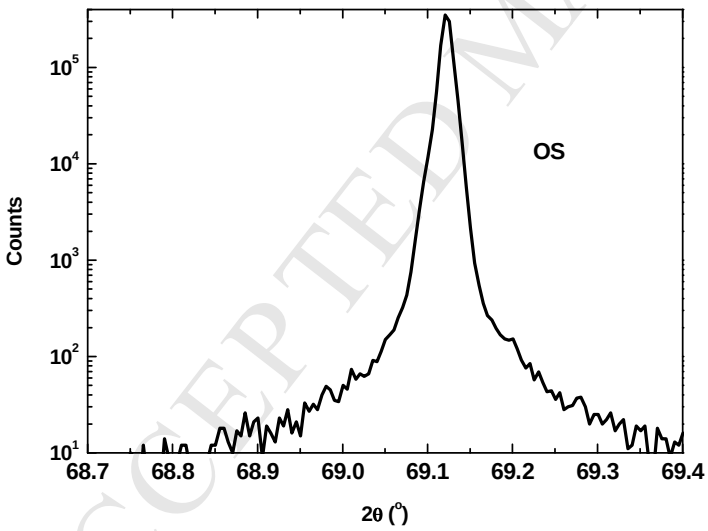

Fig.C. HRXRD of sample OS.

References

[1] Y. Son, M. Chang, H. Park, Md. S. Rahman, S. Baek, and H. Hwang, Improved electrical characteristics of fully depleted ultrathin SOI MOSFETs annealed in high pressure hydrogen ambient, Electrochem. Solid-State Lettr. 10 (2007) H324-H326.
[2] M. Bruel, Silicon on insulator material technology, Electron Lett. 31 (1995) 1201-1202 .
[3] S. Reboh, F. Rietord, L. Vignoud, F. Maze, N. Cherkashin, M. Zussy, D. Landru and C. Deuget, Effect of H-implantation in the local elastic properties of silicon crystals, Appl. Phys. Lett. 103 (2013).181911(1-5)
[4] T. Hochbauer, A. Misra, M. Nastasi, J.W. Mayer, Physical mechanisms behind the ion-cut in hydrogen implanted silicon, J. Appl. Phys., 92 (2002) 2335-2342.
[5] M. Nastasi, T. Höchbauer, J-K. Lee, A. Misra, J.P. Hirth, M. Ridgway, and T. Lafford, Nucleation and growth of platelets in hydrogen-ion-implanted silicon, Appl. Phys. Lett. 86 (2005). 154102(1-3)
[6] N. Sousbie, L. Capello, J. Eymery, F. Rieutord, and C. Lagahe, X-ray scattering study of hydrogen implantation in silicon, J. Appl. Phys. 99 (2006) 103509(1-7).
[7] D. Gu, H. Baumgart, K.K. Bourdelle, G.K. Celler, A.A. Elmustafa, Nanomechanical response of the Si lattice to hydrogen implantation and annealing for layer splitting, Jap. J. Appl. Phys. 48 (2009) 101202(1-4) .
[8] S. To, H. Wang, E.V. Jelenković, Enhancement of the machinability of silicon by hydrogenion implantation forultra-precision micro-cutting, Int. J. Mach. Tools Manuf. 74 (2013) 50-55.
[9] G.B. Xiao, S. To, E.V. Jelenković, Effects of non-amorphizing hydrogen ion implantation on anisotropy in micro cutting of silicon, J. Mater. Proc. Technol**.** 225 (2015) 439-450.
[10] E.V. Jelenković, S. To, B. Sundaravel, G.Xiao, H. Huang, Micro-cutting of silicon implanted with hydrogen and post-implantation thermal treatment, Appl. Phys. A 122 (2016) 708(1-8).
[11] J. Yan, T. Asami, H. Harada, T. Kuriyagawa, Crystallographic effect on subsurface damage formation in silicon microcutting, CRIP Ann. Manuf. Technol. 61 (2012) 131-134.
[12] Emil V. Jelenković, Suet To, Lyudmila V. Goncharova, Sing Fai Wong, Nanoindentation of silicon implanted with hydrogen: effect of implantation dose on silicon's mechanical properties and nanoindentation-induced phase transformation, Res. Mater. Express, 4 (2017) 075013(1-13).
[13] B. Aspar, H. Moriceau, E. Jalaguier, C. Lagahe, A. Soubie, B. Biasse, A.M. Papon, A. Claverie, J. Grisolia, G. Benassayag, F. Letertre, O. Rayassac, T. Barage, C. Maleville, and B. Ghyselen, The Generic Nature of the Smart-Cut® Process for Thin Film Transfer, J. Eelctr. Mater. 30 (2001) 834-840.
[14] W.C. Oliver, G.M. Pharr, Measurement of hardness and elastic modulus by instrumented indentation: advances in understanding and refinements to methodology J. Mater. Res. 19 (2004) 3-20 .
[15] M. Mayer, SIMNRA user's guide, Max-Planck-Institut fur Plasmaphysik, Garching, Germany, 1997.
[16] J. F. Ziegler, SRIM—The stopping and range of ions in matter,http://www.srim.org/
[17] H. Angelskåra, R. Søndenå, M.S. Wiig, E.S. Marsteina, Characterization of oxidation-induced stacking fault rings in Cz silicon: Photoluminescence imaging and visual inspection after Wright etch, Energy Procedia 27 (2012) 160-166.
[18] L. Chang, L. Zhang, Mechanical behaviour characterisation of silicon and effect of loading rate on pop-in: A nanoindentation study under ultra-low loads, Mater. Sci.Eng. A 506 (2009) 125-129.
[19] H. Huang, H.W. Zhao, C.L. Shi, L. Zhang, S.G Wan and C.Y Geng, Randomness and Statistical Laws of Indentation-Induced Pop-Out in Single Crystal Silicon
Materials 6 (2013), pp 1496-1505
[20] R. Sun, T Xu, Q.J. Xue, Effect of Ar+ ion implantation on the nano-mechanical properties and microstructure of single crystal silicon, Appl. Surf. Sci. 249 (2005) 386-392.

[21] D.M. Follstaedt, J.A. Knapp, and S.M. Myers, Mechanical properties of ion-implanted amorphous silicon, J. Mater. Res. 19 (2004) 338-346.
[22] D. Gu,H. Baumgart, K.K. Bourdelled, G. Celler,and A.A. Elmustafa, Weakening of hardness and modulus of the Si lattice by hydrogen implantation for layer transfer in wafer bonding technology, 214th ECS Meeting, Abstract #2209 (2008).
[23] Y. Yamashita, F. Jyobe, Y. Kamiura, and K. Maeda, Hydrogen enhanced dislocation glides in silicon, Phys. Stat. Sol. (a) 171 (1999) 27-34.
[24] X. Guo, S. Momota, N. Nittac, T. Yamaguchi, N. Sato, H. Tokaji, Modification of mechanical properties of Si crystal irradiated by Kr-beam, Appl. Sur. Sci. 349 (2015) 123-128.
[25] B. Pantchev, P. Danesh, J. Wizorek and B. Schmidt, Nanoindentation-induced pile-up in hydrogenated amorphous silicon, 2010 J. Phys: Conf. Ser. 253 (2010) 012054(1-6).
[26] P. Danesh, B. Pantchev, J. Wiezorek, B. Schmidt, Effect of hydrogen on hardness of amorphous silicon, Appl Phys A, 102 (2011) 131–135.
[27] C. Miclaus, M.S. Goorsky, Strain evolution in hydrogen-implanted silicon, J. Phys. D Appl. Phys. 36 (2003) A177–A180.
[28] B. E. Deal, The Oxidation of silicon in dry oxygen, wet oxygen, and steam, J. Electrochem. Soc. 110 (1963) 527-533.
[29] W. Düngen, R. Job, Y. Ma, Y. L. Huang, T. Mueller, Thermal evolution of hydrogen related defects in hydrogen implanted Czochralski silicon investigated by Raman spectroscopy and atomic force microscopy, J. Appl. Phys. 100 (2006) 034911(1-5).